Proceedings of the 2022
29th International Conference on Nuclear Engineering
ICONE29
August 8-12, 2022, Virtual, Online

ICONE29-92587

3-D RADIATION FIELD RECONSTRUCTION FOR A FACILITY WITH MULTIPLE RADIOACTIVE SOURCES

Shangzhen Zhu, Xinwen Dong, Shuhan Zhuang, Sheng Fang, Jianzhu Cao, Wenqian Li

Institute of Nuclear and New Energy Technology, Collaborative Innovation Centre of Advanced Nuclear Energy Technology, Key Laboratory of Advanced Reactor Engineering and Safety of Ministry of Education, Tsinghua University, Beijing, 100084, China

ABSTRACT

The radiation field measurement and surveying play important roles in optimizing and planning operation work in the radioactive area. In this work, a 3-D radiation field reconstruction method is applied to reconstruct a 3-D radiation field of a facility with two radioactive drums and a shielding, not limited to the existing methods under two-dimensional grids. A numerical scheme of the method is introduced. Monte Carlo simulation of the gamma radiation field was performed to be an original field so that the reconstruction results can be verified. Random and regular sampling ways are taken into consideration while the sampling rates are kept at 4.12%. Quantitative evaluation of the results evaluates MSE(mean relative error) and MRE(mean squared error), MRE is kept at less than 4%, which shows a good reconstruction accuracy of the method in almost all 3D space. The work in this paper has good reference value for applications such as radiation field detection, inversion, and reconstruction, operations under radioactive environments like nuclear waste decommissioning, and nuclear power radiation modeling.

Keywords: Gamma radiation field, Three-dimensional reconstruction, Simulations and verifications with multiple sources.

1. INTRODUCTION

The three-dimensional (3-D) gamma radiation field is important for optimizing and planning operation work in the radioactive area to achieve the goal of ALARA (As Low As Reasonably Achievable) [1] in applications in nuclear energy such as nuclear facility decontamination and decommissioning[2]. Radiation detectors can measure the gamma radiation field strength at a single position[3], and the deployment of detectors is usually sparse. To obtain the detailed 3-D gamma radiation field, computational methods are paid attention to, including forward and inverse methods.

The point kernel method, discrete ordinates method, and Monte Carlo (MC) method[4-6]are common forward methods and are used to compute the detailed radiation field while considering complex nuclear facility geometry and source terms. The Monte Carlo method is the most widely used and has mature program codes[7-9] such as FLUKA, MCNP, and GEANT4.

However, when the radioactive sources are unknown and the measurements are limited, the forward method may be challenging to realize the radiation field. In comparison, the inverse method can estimate radiation fields reasonably, in which interpolation algorithms and neural network methods were investigated. A 2D simple radiation field by a method based on net function interpolation to and is further improved its accuracy with Bayesian inference [10-11]. A neural network model with the inverse distance weighting method is constructed to calculate the radiation field [12]. A radiation reconstruction method based on Back-propagation (BP) neural network with decaying learning rate is proposed[13]. However, these methods have given results in 2-D radiation fields but not 3-D cases, which may restrict their applications. For 3-D radiation field reconstruction, a method using the modified Cahn-Hilliard equation[14] showed good accuracy away from the source and has been applied to simulations in separated areas of a real radioactive waste processing facility with a single radiation source. The accuracy and feasibility of the method in whole facility space and for multiple radioactive sources are still valuable for research.

This paper investigated the radiation field reconstruction performance of the method based on the modified Cahn-Hilliard (C-H) equation in the case that the facility has two radioactive sources and a shielding. The reconstruction is verified against Monte Carlo simulation results based on a real radioactive waste processing facility at the institute of nuclear and new energy technology (INET) of Tsinghua University [15-16] in China. The method is applied with 4.12% of the simulation data for the case to reconstruct the field. The reconstruction results are evaluated qualitatively and quantitatively.

2. METHODS

This section presents the theory and numerical solution of the reconstruction method, verification case, sampling ways, and evaluation ways.

2.1 Theory

To reconstruct the 3-D gamma radiation field, the method based on the modified Cahn-Hilliard equation proposed in the previous work [14] is used. The equation used is formulated as:

$$u_t = -\Delta\left(\epsilon\Delta u - \frac{1}{\epsilon}\nabla\cdot\left(\frac{\nabla u}{|\nabla u|}\right)\right) + \lambda(x)(f-u) \quad (1)$$

where $u = u(x)$ is the 3-D dose rate filed to be solved, u_t is $u(x)$ evolving in time, and $f=f(x)$ is the limited and sparse measurements (In this paper, sampled data), ϵ is the parameter determining the steepness of the transition, $\epsilon>0$. ∇ is the gradient operator and $\nabla\cdot\left(\frac{\nabla u}{|\nabla u|}\right)$ is the curvature function.

$\lambda(x)(f-u)$ is the fidelity term keeping the solution consistent with measurements. $\lambda(x)$ is the spatially varied regularization parameter, defined as:

$$\lambda(x) = \begin{cases} 0, & x \in D \\ \lambda_0, & x \in \Omega \backslash D \end{cases} \quad (2)$$

where Ω is the total region, $D \subset \Omega$ is the missing region, $\Omega\backslash D$ is the region where measurements are at.

As Eq.(1) evolves, the level lines continue smoothly into the missing domain [17] and the missing radiation field information is recovered.

2.2 Verification

The reconstruction result is verified against a Monte Carlo simulation case, which is based on the experiments[15-16] performed in a real radioactive liquid waste processing facility at the Institute of Nuclear and New Energy Technology (INET) of Tsinghua University, China. In the facility, two intermediate-level radioactive waste (ILW) drums are placed on a sliding track and are separated by a movable shielding. The geometry is shown in Fig.1. The drums are filled with cement, Cs-137 and Sr-90. The size of the simulated 3-D radiation field is 11 m in length, 2.6 m in width, and 3.5 m in height, and coordinates -300 cm to 800 cm of X-axis, -100 cm to 160 cm of Y-axis, -50 cm to 300 cm of Z-axis. Monte Carlo simulation is conducted with FLUKA, the total number of transport particles is 1e9, and other Monte Carlo simulation parameters follow the previous study [16].

The software SimpleGEO (http://www.fluka.org/fluka.php) is used to present the radiation field results by the representative slices of the reconstructed 3-D radiation field results and 3-D displays.

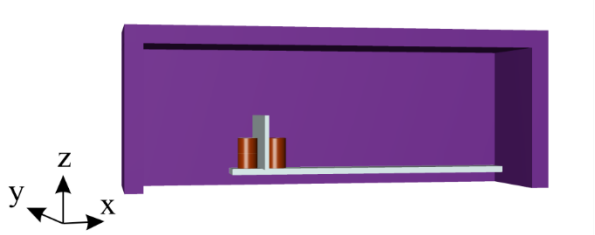

FIGURE 1: GEOMETRY MODEL OF SIMULATED FACILITY WITH RADIOACTIVE DRUMS AND SHIELDING

2.3 Sampling of input data

The simulated 3-D radiation field data are sampled randomly and regularly as the input of the reconstruction (Fig. 2). Two sets of sampled data involve less than 4.12% of the total data. The sampled data cover the accessible area in the room.

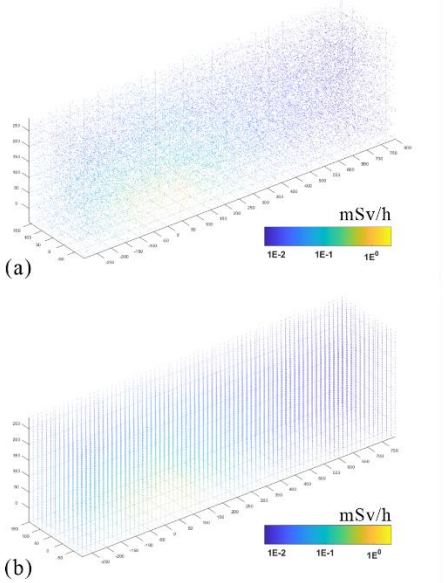

FIGURE 2: DISTRIBUTION AND STRENGTH OF SAMPLES. (a) RANDOM SAMPLING (b) REGULAR SAMPLING

2.4 Implementation: Numerical solution

The numerical implementation scheme of the discretized Eq. (1) is translated as:

$$\frac{U_{N+1}-U_N}{\Delta t} + \epsilon\Delta\Delta U_{N+1} - C_1\Delta U_{N+1} + C_2 U_{N+1} = \frac{1}{\epsilon}\Delta C(U_N) + \lambda(f-U_N) - C_1\Delta U_N + C_2 U_N \quad (3)$$

Where, $C_1 > \frac{1}{\epsilon}$, $C_2 > \lambda_0$. U_N is the discretized $u(x)$ at the N-th iteration. The fast Fourier transform (FFT) is used to accelerate the solution, and the corresponding numerical scheme of Eq. (3) is formulated as:

$$\widehat{U}_{N+1}(i,j,k) = \frac{\left(1 - C_1\Delta t\left(\frac{1}{\Delta x^2}\lambda_i + \frac{1}{\Delta y^2}\lambda_j + \frac{1}{\Delta z^2}\lambda_k\right) + C_2\Delta t\right)\widehat{U}_N(i,j,k) + \frac{\Delta t}{\epsilon}\Delta\widehat{C(U_N)}(i,j,k) + \Delta t\lambda\widehat{(f-U_N)}}{1 + C_2\Delta t + \epsilon\Delta t(\frac{1}{\Delta x^2}\lambda_i + \frac{1}{\Delta y^2}\lambda_j + \frac{1}{\Delta z^2}\lambda_k)^2 - C_1\Delta t(\frac{1}{\Delta x^2}\lambda_i + \frac{1}{\Delta y^2}\lambda_j + \frac{1}{\Delta z^2}\lambda_k)} \quad (4)$$

Where, $\hat{U}$ is the FFT of U with eigenvalues λ_i. The iteration of Eq. (4) performed 1000 steps for reconstructions with random and regular samplings.

2.5 Performance Evaluation

To evaluate the performance of 3-D gamma radiation field reconstruction, MRE (mean relative error) and MSE (mean squared error) are computed. The formulae of MRE and MSE are as follows:

$$MRE = \frac{\sum_i^n \frac{|R_i - A_i|}{A_i}}{n} \quad (5)$$

$$MSE = \sum_i^n \frac{(R_i - A_i)^2}{n} \quad (6)$$

Where A_i is the actual value and R_i reconstructed value, n is the number of reconstruction grid points.

3. RESULTS AND DISCUSSION

Showed in Fig. 3a, the distribution of the radiation field is symmetrical on both sides of the shield because of the consistent radioactive drums. A radiation peak at higher levels appears above the iron shielding because of the sum of the radiation dose rates contributed by the two drums. The minimal dose rate locates in the deep space near the inner wall. The maximal dose rates of the radiation field appear near the surface of the drums over 3.0 mSv/h on both sides of the shielding. The overall reconstruction results are displayed in Fig.3. The representative slices and their comparisons are displayed in Fig.4 and Fig.4 use the same color bar as Fig.3. Three sections intersect at 0 cm of the X-axis, 0 cm of the Y-axis, 0 cm of the Z-axis.

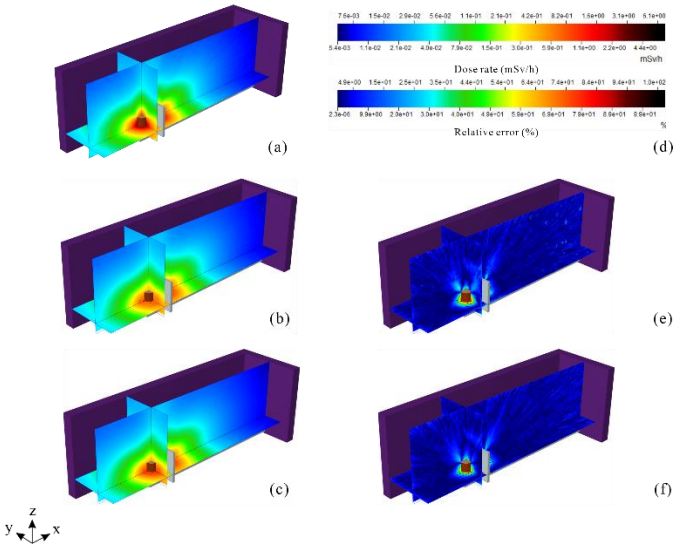

FIGURE 3: THE 3-D DISPLAY OF MONTE CARLO SIMULATION AND RECONSTRUCTION RESULTS (a)MC SIMULATION RESULT. (b) RECONSTRUCTION RESULT (RANDOM SAMPLING) (c) RECONSTRUCTION RESULT (REGULAR SAMPLING) (d) COLORBAR (e) RELATIVE ERROR MAP (RANDOM SAMPLING) (f) RELATIVE ERROR MAP (REGULAR SAMPLING)

For reconstruction with random samplings, the reconstructed radiation field agrees with the MC simulation in most areas on the radiation strength distribution in the whole 3-D domain. However, in the reconstructed field, the maximal dose rates are lower than in the original simulation radiation field. The relative error map shows that the maximal dose rates near the space lose to the drums in the reconstructed field are about 30~70% lower than those in the original field. Other than that, Both the radiation dose rates match the variation of more than two orders of magnitude of the MC simulation. Fig.3e shows that the relative error between the reconstruction and MC simulation is highly low in most of the space, less than 4.9% in the vast majority of areas. The higher relative errors gather near the drums, which is because of sharp dose rate decay near the drums and the higher relative error dramatically decreases below 30% 0.25 meters from the surface of the drum.

The more detailed section displays are shown in Fig.4. The top view shows the symmetrical radiation field intensity distribution on both sides of the shield, and the intensity decreases isotropically around sources. The front view also shows the reconstructed radiation field agrees with the original field and the reconstruction shows more smooth distribution in the large distance because the little sparse samples near the drums are challenging to capture the steep gradient change near drums in small area. The left view displays similar features to the front view. All error maps in three views show low relative error in most areas but space near the drums. The higher relative error near the drum surface is still within one fold.

For reconstruction with regular samplings, the reconstructed radiation field agrees with the MC simulation field, and have low relative errors in most area and higher relative error in space near the drum, similar to the reconstruction result using random samplings. Showed in Fig. 3f, there is a decrease in the higher relative error near the drum by over 10% and shows that regular samplings may help the reconstruction capture the big and isotropic gradient change more efficiently. The detailed section displays also show a relative error decrease near the space close to the drums compared to reconstruction using random samplings. All views show low relative error less than 4.9% in the majority of space in the facility.

Table 1 summarizes MSE and MRE of the reconstruction results. Reconstruction using two sampling ways has similar performance. The MRE values of 3-D reconstructions are all good, below 3.75%, showing the accuracy and usability of the method in the case of multiple sources.

Table 1: MSE AND MRE OF RECONSTRUCTION RESULTS

Sampling way	MSE (mSv^2/h^2)	MRE (%)
Random sampling	4.1883e-03	3.75
Regular sampling	4.3154e-03	3.63

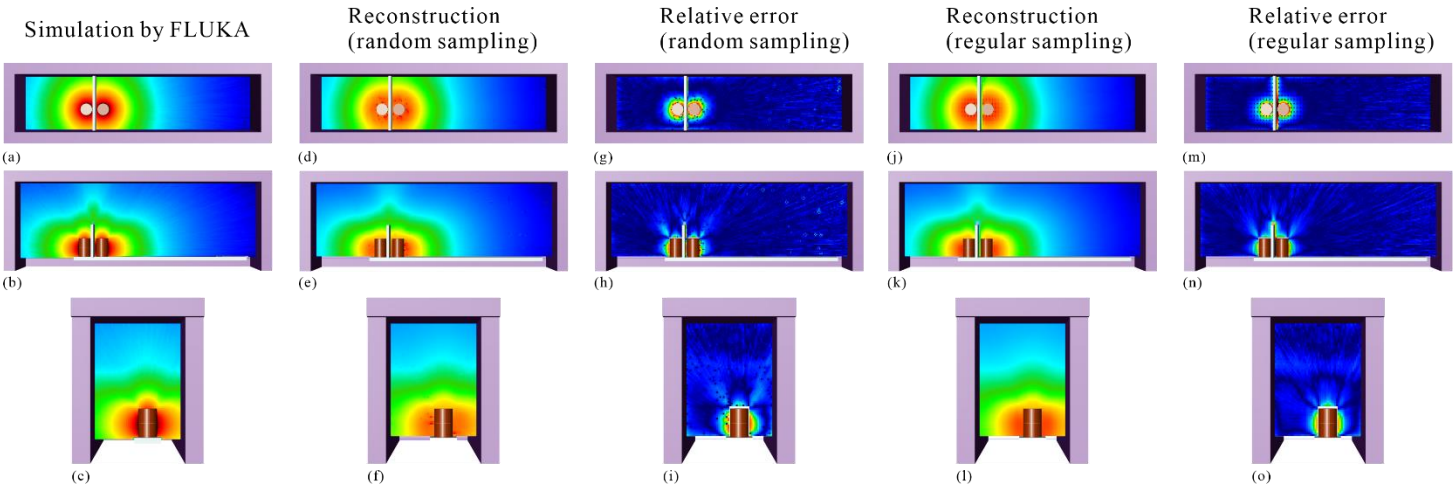

FIGURE 4: THE SECTION DISPLAYS OF COMPARISON BETWEEN MONTE CARLO SIMULATIONS AND RECONSTRUCTION RESULTS (a) (b) (c)MC SIMULATION RESULT. (d) (e) (f) RECONSTRUCTION RESULT (RANDOM SAMPLING) (j) (k) (l) RECONSTRUCTION RESULT (REGULAR SAMPLING) (g) (h) (i) RELATIVE ERROR MAP (RANDOM SAMPLING) (m) (n) (o) RELATIVE ERROR MAP (REGULAR SAMPLING)

4. CONCLUSION

This work applied a 3-D radiation field reconstruction method to reconstruct a 3-D radiation field of a real radioactive waste processing facility with two radioactive drums and a shielding. The theory and numerical scheme of the method are introduced. The feasibility and accuracy of the method are verified by comparing the reconstruction results with the Monte Carlo simulation field. Random and regular sampling ways are used and the sampling rate is 4.12%. Quantitative and qualitative evaluations of the results are performed. MREs of results are less than 3.8%.

ACKNOWLEDGEMENTS

This work is supported by the National Natural Science Foundations of China [grant number 11875037], International Atomic Energy Agency (TC project number CRP9053) and the foundation of Key Laboratory of Advanced Reactor Engineering and Safety, Ministry of Education [grant number ARES-2018-08].

REFERENCES

[1] ICRP, 1991. Recommendations of the International Commission on Radiological Protection. ICRP Publication 60. Ann. ICRP 21(1–3).

[2] Ilg, P., Gabbert, S., Weikard, H.-P., 2017. Nuclear Waste Management under Approaching Disaster: A Comparison of Decommissioning Strategies for the German Repository Asse II. Risk Analysis 37, 1213–1232. https://doi.org/10.1111/risa.12648

[3] Knoll, G.F., 1979. Radiation detection and measurement, New York.

[4] Prokhorets, I.M., Prokhorets, S.I., Khazhmuradov, M.A., Rudychev, E.V., Fedorchenko, D.V., 2007. Point Kernel method for radiation fields simulation. Probl. At. Sci. Technol. 48, p.106.

[5] Lacoste, V., Gressier, V., Institut de Radioprotection et de Sûreté Nucléaire, 2004. Monte Carlo simulation of the IRSN CANEL/T400 realistic mixed neutron-photon radiation field. Radiat Prot Dosimetry 110, 123–127. https://doi.org/10.1093/rpd/nch190

[6] Lux, I., Koblinger, L., 2017. Monte Carlo Particle Transport Methods: Neutron and Photon Calculations. CRC Press, Boca Raton. https://doi.org/10.1201/9781351074834

[7] Ferrari, A., Sala, P.R., Fasso, A., Ranft, J., 2005. FLUKA: A Multi-Particle Transport Code (No. SLAC-R-773, 877507). https://doi.org/10.2172/877507

[8] Pelowitz, D.B., 2008. MCNPX User's Manual, Version 2.6.0. Los Alamos National Laboratory Report LA-CP-07-1473.

[9] Agostinelli, S., Allison, J., Amako, K., Apostolakis, J., Araujo, H., Arce, P., Asai, M., Axen, D., Banerjee, S., Barrand, G., Behner, F., Bellagamba, L., Boudreau, J., Broglia, L., Brunengo, A., Burkhardt, H., Chauvie, S., Chuma, J., Chytracek, R., Cooperman, G., Cosmo, G., Degtyarenko, P., Dell'Acqua, A., Depaola, G., Dietrich, D., Enami, R., Feliciello, A., Ferguson, C., Fesefeldt, H., Folger, G., Foppiano, F., Forti, A., Garelli, S., Giani, S., Giannitrapani, R., Gibin, D., Gómez Cadenas, J.J., González, I., Gracia Abril, G., Greeniaus, G., Greiner, W., Grichine, V., Grossheim, A., Guatelli, S., Gumplinger, P., Hamatsu, R., Hashimoto, K., Hasui, H., Heikkinen, A., Howard, A., Ivanchenko, V., Johnson, A., Jones, F.W., Kallenbach, J., Kanaya, N., Kawabata, M., Kawabata, Y., Kawaguti, M., Kelner, S., Kent, P., Kimura, A., Kodama, T., Kokoulin, R., Kossov, M., Kurashige, H., Lamanna, E., Lampén, T., Lara, V., Lefebure, V., Lei, F., Liendl, M., Lockman, W., Longo, F., Magni, S., Maire, M., Medernach, E., Minamimoto, K., Mora de Freitas, P., Morita, Y., Murakami, K., Nagamatu, M., Nartallo, R., Nieminen, P., Nishimura, T., Ohtsubo, K., Okamura, M., O'Neale, S., Oohata, Y., Paech, K., Perl, J., Pfeiffer, A., Pia, M.G., Ranjard, F., Rybin, A., Sadilov, S., Di Salvo, E., Santin, G., Sasaki, T., Savvas, N., Sawada, Y., Scherer, S., Sei, S., Sirotenko, V., Smith, D., Starkov, N., Stoecker, H., Sulkimo, J., Takahata, M., Tanaka, S., Tcherniaev,

E., Safai Tehrani, E., Tropeano, M., Truscott, P., Uno, H., Urban, L., Urban, P., Verderi, M., Walkden, A., Wander, W., Weber, H., Wellisch, J.P., Wenaus, T., Williams, D.C., Wright, D., Yamada, T., Yoshida, H., Zschiesche, D., 2003. Geant4—a simulation toolkit. Nuclear Instruments and Methods in Physics Research Section A: Accelerators, Spectrometers, Detectors and Associated Equipment 506, 250–303. https://doi.org/10.1016/S0168-9002(03)01368-8

[10] Wang, Z., Cai, J., 2020. Reconstruction of the neutron radiation field on nuclear facilities near the shield using Bayesian inference. Progress in Nuclear Energy 118, 103070. https://doi.org/10.1016/j.pnucene.2019.103070

[11] Wang, Z., Cai, J., 2018. Inversion of radiation field on nuclear facilities: A method based on net function interpolation. Radiation Physics and Chemistry 153, 27–34. https://doi.org/10.1016/j.radphyschem.2018.09.003

[12] Li, M.-K., Liu, Y.-K., Peng, M.-J., Xie, C.-L., Yang, L.-Q., 2018. A fast simulation method for radiation maps using interpolation in a virtual environment. J. Radiol. Prot. 38, 892–907. https://doi.org/10.1088/1361-6498/aac392

[13] Zhou, W., Sun, G., Yang, Z., Wang, H., Fang, L., Wang, J., 2021. BP neural network based reconstruction method for radiation field applications. Nuclear Engineering and Design 380, 111228. https://doi.org/10.1016/j.nucengdes.2021.111228

[14] Zhu, S., Cao, J., Fang, S., Dong, X., Li, W., Liu, X., He, Q., Wang, X., 2022. 3-D gamma dose rate reconstruction for a radioactive waste processing facility using sparse and arbitrarily-positioned measurements. Progress in Nuclear Energy 144, 104073. https://doi.org/10.1016/j.pnucene.2021.104073

[15] Li, W., Liu, X., Li, M., Huang, Y., Fang, S., 2019. Multilayer Shielding Design for Intermediate Radioactive Waste Storage Drums: A Comparative Study between FLUKA and QAD-CGA. Science and Technology of Nuclear Installations 2019, e8186798. https://doi.org/10.1155/2019/8186798

[16] Li, W., Liu, X., Fang, S., Fu, X., Guo, K., 2020. Monte Carlo Simulation and Experimental Validation for Radiation Protection with Multiple Complex Source Terms and Deep Penetration for a Radioactive Liquid Waste Cementation Facility. Science and Technology of Nuclear Installations 2020, 8819794. https://doi.org/10.1155/2020/8819794

[17] Schönlieb, C.-B., 2015. Partial Differential Equation Methods for Image Inpainting, Cambridge Monographs on Applied and Computational Mathematics. Cambridge University Press, Cambridge. https://doi.org/10.1017/CBO9780511734304